Statistical Assessment of the OWZ Tropical Cyclone Tracking Scheme in ERA-Interim

SAMUEL S. BELL AND SAVIN S. CHAND

Faculty of Science and Technology, Federation University, Ballarat, Victoria, Australia

KEVIN J. TORY

Research and Development Branch, Bureau of Meteorology, Melbourne, Victoria, Australia

CHRISTOPHER TURVILLE

Faculty of Science and Technology, Federation University, Ballarat, Victoria, Australia

(Manuscript received 14 August 2017, in final form 10 November 2017)

ABSTRACT

The Okubo–Weiss–Zeta (OWZ) tropical cyclone (TC) detection scheme, which has been used to detect TCs in climate, seasonal prediction, and weather forecast models, is assessed on its ability to produce a realistic TC track climatology in the ERA-Interim product over the 25-yr period 1989 to 2013. The analysis focuses on TCs that achieve gale-force ($17\,m\,s^{-1}$) sustained winds. Objective criteria were established to define TC tracks once they reach gale force for both observed and detected TCs. A lack of consistency between storm tracks preceding this level of intensity led these track segments to be removed from the analysis. A subtropical jet (STJ) diagnostic is used to terminate transitioning TCs and is found to be preferable to a fixed latitude cutoff point. TC tracks were analyzed across seven TC basins, using a probabilistic clustering technique that is based on regression mixture models. The technique grouped TC tracks together based on their geographical location and shape of trajectory in five separate ''cluster regions'' around the globe. A mean trajectory was then regressed for each cluster that showed good agreement between the detected and observed tracks. Other track measures such as interannual TC days and translational speeds were also replicated to a satisfactory level, with TC days showing limited sensitivity to different latitude cutoff points. Successful validation in reanalysis data allows this model- and grid-resolution-independent TC tracking scheme to be applied to climate models with confidence in its ability to identify TC tracks in coarse-resolution climate models.

1. Introduction

Tropical cyclones (TCs) often have devastating social and economic impacts that may be exacerbated in the future as a result of anthropogenically induced climate change. This has attracted a widespread scientific investigation into the area of TC projections and climate change (e.g., Walsh et al. 2016). Future projections of TCs are often provided by climate models, particularly those from the most recent Coupled Model Intercomparison Project (CMIP5; Taylor et al. 2012). As these models typically have coarse horizontal resolutions of approximately 100–300 km, they are unable to resolve the fine structure of a TC-like circulation. Therefore, to identify and track TCs in climate-model-simulated data, a ''TC detector'' must be used. Currently, there is no accepted ''gold standard'' detector to use; different detectors have strengths and weaknesses and can produce different results when applied to the same model (e.g., Horn et al. 2014). This elevates the need for a model- and resolution-independent metric for improved TC detection and tracking in climate models and for more consistent TC projection results.

Generally, all detectors seek to identify TCs by identifying expected anomalies in storm-system-scale [$O(10^3)$ km] atmospheric quantities, such as relative vorticity or low-level temperature. Traditional detectors (e.g., Bengtsson et al. 1995; Chauvin et al. 2006; Strachan et al. 2013) also include finer-scale parameters (such as a dip in central pressure or maxima of wind thresholds) to

Corresponding author: Samuel S. Bell, ss.bell@federation.edu.au

DOI: 10.1175/JCLI-D-17-0548.1

identify TCs directly, which causes a reliance of the detector on model and grid resolution (Walsh et al. 2007). This results in a selected threshold value of a parameter having to be used to tune the detector to best reproduce the observed TC climatology. As models often have their own dedicated detector, comparisons between models become limited as it is difficult to isolate the model errors from the detection errors (Tory et al. 2013b, hereinafter T13B; Horn et al. 2014). In turn, the ability to obtain robust conclusions from a suite of models regarding future TC projections is degraded (e.g., Camargo 2013; Daloz et al. 2015).

Recently Tory et al. (2013a, hereinafter T13A) sought to overcome this limitation with a more indirect detection approach, where environments favorable to TC development are used to identify TCs. This approach allows strictly storm-system-scale parameters to be used for detection.

Key points on this detector include the following:

- The detector was tuned in ERA-Interim data at a similar resolution as would be applied to the current generation of CMIP models,[1] thereby reducing grid- and model-resolution dependence on the choice of parameter thresholds (Tory et al. 2013d, hereinafter T13D).
- Formulation of this detector focused on identifying circulations with characteristics that favor TC-scale vortex intensification. Most notably, the Okubo–Weiss–Zeta (OWZ; T13A) variable is used in place of the commonly used relative vorticity in order to more closely pinpoint the TC formation sweet spot (Dunkerton et al. 2009).
- Other thresholds include humidity fields and the limiting factor of vertical wind shear (VWS), which are all atmospheric variables resolvable in coarse-resolution climate model outputs.
- Identified circulations are linked in time to produce tracks.

Hereafter both the detection and tracking components are referred to together as the OWZ scheme, while the terms OWZ detector (OWZ-D) and OWZ tracker (OWZ-T) are used to refer to different components of the scheme separately.

[1] The ERA-Interim data were originally downloaded at a 1.5° horizontal grid spacing and then regridded at a 1.0° grid spacing in order to best replicate the intended procedure of regridding coarse-resolution climate model data to a common grid. Later the analysis was repeated using data downloaded at a 1.0° grid spacing, which yielded a small improvement in detection performance (e.g., Tory et al. 2018). Tracks from the latter analysis are used in this study.

The OWZ scheme first identifies circulations that have some potential for TC formation, using relatively weak thresholds in an attempt to identify all observed TC tracks. The storm tracks are then assessed (OWZ-D) as to whether they meet the criteria for a TC, which occurs for about 10%–15% of the tracks. Note that we refer to storms that exceed gale-force intensity hereafter as a TC, in accordance with the Australian–South Pacific definition of the term. While the number and approximate genesis location of OWZ scheme detections has been verified (T13B), and allowed for extensive application of the scheme in genesis-related studies over the last five years (Tory et al. 2013c,d, 2014, 2018), the TC tracks (i.e., track preceding and occurring after TC genesis) have yet to be validated. The validation of these tracks therefore forms the basis of this paper. Evaluating projected changes in TC tracks in a warming climate is crucial, particularly if it involves assessing local-scale impacts, such as TC landfall positions. Likewise, changes in other track characteristics such as TC days are also important. However, before the tracking scheme can be confidently applied to climate model data, it is first important to verify that it can reproduce a realistic TC track climatology from a global reanalysis product. The application of the OWZ scheme to reanalysis data will give an overall evaluation of biases associated with the scheme and will provide opportunities to implement appropriate statistical corrections (if necessary) before it is applied to climate model simulations.

Our paper is structured as follows. Data, definitions, and methodology are discussed in section 2. Section 3 presents an analysis of track cutoff points and establishes criteria to objectively split each track into two segments. Section 4 provides a detailed statistical assessment of the OWZ scheme's tracking performance in ERA-Interim data. Finally, section 5 provides a summary of key findings and concluding remarks.

2. Data and methodology

a. TC data and definitions

The International Best Track Archive for Climate Stewardship (IBTrACS; Knapp et al. 2010a,b) is a comprehensive compilation of quality-controlled global TC best-track data, available at 6-h intervals and sourced from several meteorological organizations and agencies around the world. We use the version of data that is specifically sourced from World Meteorological Organization (WMO) responsible centers (see caption of Fig. 1). In this study, TC tracks from this database are taken 12-hourly at 0000 and 1200 UTC for computational convenience over the 25-yr period 1989–2013.

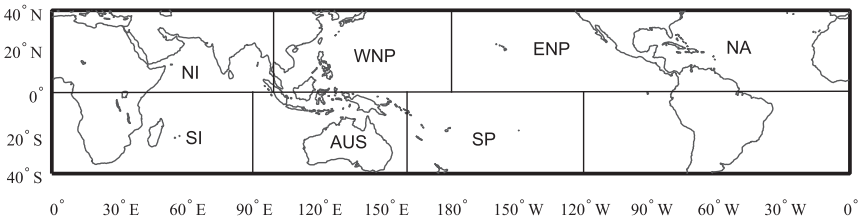

FIG. 1. The seven TC basins used in this study and the meteorological warning center(s) that observational data is taken from follows its definition: NI (0°–100°E; New Delhi), WNP (100°E–180°; Tokyo), ENP (180°–~90°W; Miami and Honolulu), NA (~90°W–0°; Miami); south Indian Ocean (SI: 0°–90°E; Réunion), Australia (AUS: 90°–160°E; Perth, Brisbane, Darwin, Jakarta, and Port Moresby), and South Pacific (SP: 160°E–120°W; Nadi and Wellington).

Data in this period are consistent with the era after which routine satellite observations became available, thus providing a consistent platform of verification for tracks detected by the OWZ scheme.

All tropical depressions from the IBTrACS database are excluded by objectively defining a TC as any system in the database that reached the 10-min maximum sustained wind of 17 m s^{-1} at either 0000 or 1200 UTC; the first such position where the wind speed exceeds 17 m s^{-1} is defined as the TC genesis point. This definition includes all systems that reached at least category 1 on the Australian tropical cyclone intensity scale (available at http://www.bom.gov.au/cyclone/about/intensity.shtml). The Australian scale is used to describe different TC "categories" in this paper; note a category 1 on this scale is equivalent to the definition of a tropical storm (e.g., National Hurricane Center). Additionally, wind speeds in the IBTrACS database for the north Indian Ocean (NI) Basin (3-min sustained) and the North Atlantic and eastern North Pacific basins (1-min sustained) are converted to 10-min sustained winds by using conversion factors of 0.95 and 0.93, respectively (Harper et al. 2010). TC tracks are terminated if they encounter an objectively diagnosed subtropical jet (STJ; Tory and Dare 2015; also see section 3a). Altogether, seven TC basins are defined (Fig. 1) and for cases where a TC crosses two basins, the first track point of that TC determines its basin.

b. *ERA-Interim*

ERA-Interim (Dee et al. 2011) is a global atmospheric reanalysis product generated by the European Centre for Medium-Range Weather Forecasts (ECMWF) available at a variety of horizontal resolutions and a vertical resolution of 50 hPa in the lower troposphere. For this study, the required atmospheric data for the OWZ-D were downloaded on a 1° × 1° grid to match a common grid that will be applied to all CMIP5 models used in our later studies. The 12-hourly atmospheric variables used to generate the OWZ-D parameters (at 0000 and 1200 UTC) are as follows:

- zonal and meridional wind components at 850- and 500-hPa levels for OWZ, as well as at 200 hPa for VWS, computations,
- relative humidity (RH) at 950 and 700 hPa,
- specific humidity (SpH) at 950 hPa, and
- in addition, the tracker uses winds at 700 hPa to calculate a TC steering flow (e.g., Chan and Gray 1982).

c. *Detection and tracking*

1) OWZ-D PARAMETERS

The OWZ variable is a low-deformation vorticity parameter (T13A) used to identify regions favorable for TC formation at the center of a semiclosed circulation (i.e., a "marsupial pouch"; Dunkerton et al. 2009), within the lower–middle troposphere. More precisely, it is the product of absolute vorticity and the Okubo–Weiss parameter (Okubo 1970; Weiss 1991) normalized by the vertical components of relative vorticity squared such that

$$\mathrm{OWZ} = \mathrm{sgn}(f) \times (\zeta + f) \times \max\left[\frac{\zeta^2 - (E^2 + F^2)}{\zeta^2}, 0\right], \tag{1}$$

where f is the Coriolis parameter, $\zeta = \partial v/\partial x - \partial u/\partial y$ is the vertical component of relative vorticity, $E = \partial u/\partial x + \partial v/\partial y$ is the stretching deformation, and $F = \partial v/\partial x + \partial u/\partial y$ is the shearing deformation. Minimum OWZ thresholds at both the 850- and 500-hPa levels are essential in recognizing the presence of a deeply organized low pressure system. However, these parameters alone are not sufficient to discriminate environments that support TC formation from those that do not. Hence,

TABLE 1. Parameter threshold values for the two sets of the OWZ-D's detection criteria; subscripts refer to pressure level in hectopascals.

	OWZ-D parameter thresholds					
Criterion	OWZ_{850}	OWZ_{500}	RH_{950}	RH_{700}	$VWS_{850–200}$	SpH_{950}
Initial	$50 \times 10^{-6}\,s^{-1}$	$40 \times 10^{-6}\,s^{-1}$	70%	50%	$25\,m\,s^{-1}$	$10\,g\,kg^{-1}$
Core	$60 \times 10^{-6}\,s^{-1}$	$50 \times 10^{-6}\,s^{-1}$	85%	70%	$12.5\,m\,s^{-1}$	$14\,g\,kg^{-1}$

additional dynamic and thermodynamic parameters associated with TC formation conditions are required. These include a maximum threshold of the magnitude of the difference between wind vectors at the 850- and 200-hPa levels (vertical wind shear), and minimum thresholds of 950- and 700-hPa relative humidity, and 950-hPa specific humidity (Table 1).

2) TC DETECTION AND TRACKING

TC detection in ERA-Interim primarily involves two sets of detection criteria (initial and core; see Table 1): the initial set of parametric thresholds are relatively weaker than the core set of thresholds. The OWZ-D uses the initial parametric thresholds to identify grid points that comprise components of a storm circulation; neighboring grid points are then grouped together to define circulations with potential to become TCs. These circulations are linked in time by the OWZ-T to create storm tracks, which are then tested for TC declaration using the core thresholds. When the core thresholds are satisfied for five consecutive 12-h time periods (i.e., 48 h), that circulation is declared a TC. The point on a storm track where TC declaration occurs is termed its "TC declaration point." T13A determined that this sustained minimum period of 48 h was optimal for discriminating developing from nondeveloping systems across all the TC basins. Hence, only those storm tracks containing a TC declaration are used in this study to compare against TCs in the IBTrACS database. Note that the tracker also has a land-based criterion that may prevent or delay such declarations.

The OWZ scheme is concisely summarized below, with further details accessible in T13A.

(i) Each 1° × 1° grid point is assessed based on the initial threshold values of each OWZ-D parameter every 12 h.
(ii) When at least two neighboring grid points satisfy the initial thresholds of each OWZ-D parameter, these points are considered to represent a single circulation at that point in time.
(iii) The circulations from step (ii) are linked through time by estimating their position in relation to the circulation's expected position based on an averaged 4° × 4° steering wind at 700 hPa.
(iv) Tracks are terminated when no circulation match is found in the next two time steps within a generous (~350 km) latitude-dependent radius.
(v) The core thresholds are then applied to each storm track, and if they are satisfied for five consecutive 12-h time periods a TC is declared.

d. *Track clustering method*

General track patterns are elucidated through the probabilistic regression mixture curve clustering method of Gaffney (2004), which has been successfully applied in several previous studies (e.g., Gaffney et al. 2007; Camargo et al. 2007, 2008; Chand and Walsh 2009; Kossin et al. 2010; Ramsay et al. 2012; Paliwal and Patwardhan 2013; Daloz et al. 2015). Specific implementation of the method follows prior studies (e.g., Camargo et al. 2007; Chand and Walsh 2009; Ramsay et al. 2012), where linear regression mixtures (the standard clustering method) are performed on unprocessed track data. This gives the method an edge over other clustering techniques, such as k means, in which preprocessing of track data (e.g., zeroing of track points prior to clustering) is essential. Cluster regions for the Northern Hemisphere (NH) are the same as the basins defined in Fig. 1, while the three Southern Hemisphere (SH) basins are clustered altogether with no prior splitting by basin (as in Ramsay et al. 2012).

The choice of the optimal number of clusters k is crucial for establishing overall track characteristics for the different TC regions. Log-likelihood values, which are the log probability of occurrence of different clusters, are often used to determine an ideal solution. For each region, these values are found to increase as k is increased, requiring a subjective evaluation of where the gradient appears to be "leveling off." This procedure often indicates a handful of solutions rather than any specific one. Prior studies generally base their final decision on the degree of cluster correlations with natural modes such as El Niño–Southern Oscillation (e.g., Camargo et al. 2007). However, the focus of our study is on comparing TC tracks from two different sources (IBTrACS and tracks detected in reanalysis data) rather than describing cluster-specific modulation.

TABLE 2. The five clustered regions, detailing the order of the regression curve used and the choice of No. of clusters k.

Region	Curve fit	k in this study	k in prior study	References
NA	Cubic	4	4	Kossin et al. (2010) and Daloz et al. (2015)
ENP	Quadratic	3	3	Camargo et al. (2008)
WNP	Cubic	6	6–7	Camargo et al. (2007)
NI	Quadratic	3	5	Paliwal and Patwardhan (2013)
SH	Quadratic	7	7	Ramsay et al. (2012)

It is therefore more pertinent to ensure clustered groups are stable in both these sources, when selecting an appropriate k, so that TC tracks can be accurately compared. We ensure clusters are stable by performing multiple runs of each analysis where the highest-likelihood solution is obtained from 10 starts of expected maximization (EM; Camargo et al. 2008). If significant changes were found in the mean genesis or trajectory of a cluster over these runs, it was considered "unstable." Only the cluster above Australia was found to be unstable by this criterion, because of the erratic nature of tracks here. Overall, the value of k used for similar cluster regions in prior studies are found to be quite optimal (Table 2), except for the north Indian Ocean region where a smaller value of k is used to ensure stability.

e. One-to-one track verification

Verifying TC tracks detected by the OWZ scheme in ERA-Interim data by matching them (on a one-to-one basis) with the tracks observed in the IBTrACS database adds an extra layer of validation to the study, compared with simply comparing the general patterns of all observed and detected tracks. Proportions of success (i.e., rates of matching systems) are covered in T13B, while for this study we extend this analysis with the inclusion of tracks allowing for a more rigorous examination of these measures.

A simple TC track verification scheme (Table 3) is implemented where tracks can be categorized as either hits, misses, or false alarms.

- Tracks are verified as hits if on the date and time an observed TC in IBTrACS reaches its maximum intensity there is a match within the full track of a TC detected in ERA-Interim on the corresponding date and time within a 3.5° radius. Note that 98% occur within a 2° radius (i.e., a TC detected by the OWZ scheme is found to correspond to an observed TC from the IBTrACS database, with both deemed hits).
- TCs in IBTrACS that have no match are considered misses.
- Similarly, unmatched TCs detected in ERA-Interim by the OWZ scheme are considered false alarms.

Although the 3.5° hit radius may seem quite large, it is justified because of the following reasons:

1) The OWZ-D identifies the circulation position as the center of the region of satisfied thresholds, which coincides with the center of overlapping parts of the circulations between 850 and 500 hPa. For a tilted storm, this could deviate substantially from the low-level circulation center.
2) Data assimilation does not always put storms in the right place.
3) Increasing the radius from 2° to 3.5° does not produce erroneous hits.

3. Objective track definitions

This brief section details the chosen track cutoff point and gives clarity on track definitions necessary for the upcoming analysis (following this section). The focal point here is the global analysis of TC tracks with different segments highlighted (Fig. 2) as observed in IBTrACS and as detected by the OWZ scheme in ERA-Interim data.

a. Importance of the STJ cutoff

As the OWZ scheme was not designed to monitor the storm structure of a TC after it has been declared, storms may (or may not) continue to be tracked after they have transitioned to become extratropical storms. For this reason our analysis employs an STJ diagnostic, where STJs are diagnosed by a 200-hPa jet stream $>25\,\mathrm{m\,s^{-1}}$ and zonal winds exceeding $15\,\mathrm{m\,s^{-1}}$ (T13D), to terminate both the observed and detected tracks at an objectively determined subtropical location (i.e., where a TC is situated poleward of an STJ). This, of course, is under the assumption that if TCs are to encounter the

TABLE 3. Contingency table used for track verification.

	Observed	
Detected	Yes	No
Yes	Hit	False alarm
No	Miss	Correct rejection

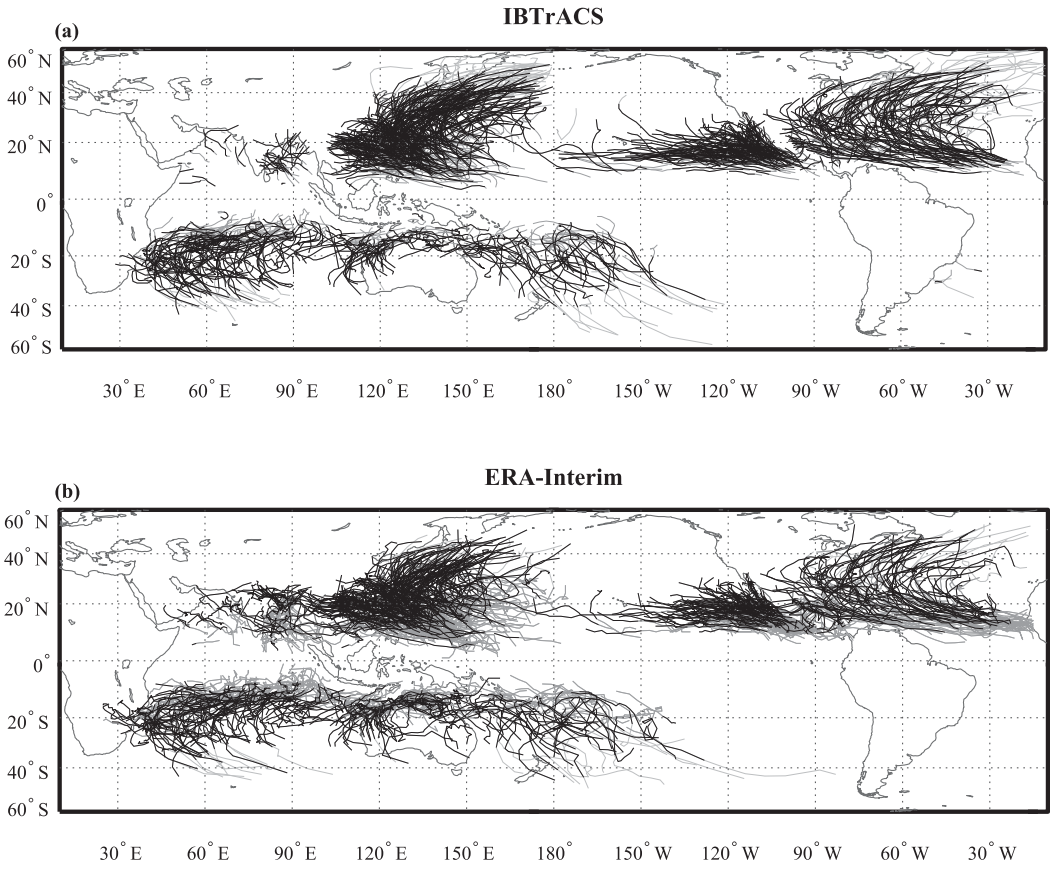

FIG. 2. Tracks of TCs from 2003 to 2013 (a) observed in the IBTrACS database and (b) detected in ERA-Interim data. The overlaid black tracks (TC tracks) are simply highlighted sections of the gray tracks that show where TCs are terminated if they cross the STJ and where the TC genesis point in (a) and the TC declaration point in (b) are located.

STJ they are likely to no longer be tropical in nature (see T13D; Tory and Dare 2015). That is, the TC is potentially sourcing a large proportion of its energy from the release of baroclinic instability. This approach differs from other track studies that either implement a fixed latitude cutoff of around 30°–40° or none at all (e.g., Table 1 in Chauvin et al. 2006).

Here, we look to document what differences an STJ cutoff makes to a more traditional cutoff point of 40° latitude. But we first give a caveat that the STJ diagnostic is not perfect, and that STJs are not always present in the real atmosphere. Inevitably, this means some high-latitude storm tracks will remain in the database. Geographical position of termination by the STJ for both observed and detected tracks are identified by the beginning of the light-gray track segments in Fig. 2 (segments nearer the poles). Focusing on the observations (Fig. 2a), it is visually clear that the STJ cuts off TC tracks mostly well before they reach 40°S in the SH. In contrast, TC tracks in the NH regularly extend beyond 40°N, particularly in the western North Pacific (WNP) and North Atlantic (NA) basins. The general latitude of where the STJ suggests a storm is transitioning (Fig. 2) is in agreement with studies on the topic matter. For example, Sinclair (2002) found a high rate of transitioning storms slightly north of New Zealand in the South Pacific. Similarly, Hart and Evans (2001) found that TCs in the North Atlantic are most likely to transition between the latitudes of 35° and 45°N. Meanwhile, TCs in the eastern North Pacific (ENP) rarely track beyond 30°N (e.g., Romero-Vadillo et al. 2007) and seldom undergo subtropical transition.

Comparisons of the percentage of track points removed in an STJ cutoff and a 40° latitude cutoff are found to be quite similar (Table 4). Overall, we prefer the STJ cutoff as it provides an objective, dynamically based definition of the ‘‘tropical edge,’’ which can account for the possibility of an expansion of the tropics in future climate scenarios (e.g., Kossin et al. 2014).

TABLE 4. Percentage of track points removed if they are poleward of the STJ or a fixed 40° latitude cutoff point in IBTrACS and the ERA-Interim.

	IBTrACS		ERA-Interim	
Hemisphere	STJ	40° lat	STJ	40° lat
SH	5%	2%	4.5%	1.5%
NH	8.5%	8%	2.5%	3.5%

b. Track definitions

Note that hereinafter, unless explicitly stated, all tracks under discussion and to be analyzed have been terminated if they encounter the STJ (i.e., the light-gray segments showing where an STJ cut off a track are no longer considered to be part of a "full track"). We make the following definitions.

- "Initial track" refers to the track that precedes TC genesis (first track point $>17\,\mathrm{m\,s^{-1}}$) in IBTrACS (Fig. 2a) and the track that precedes the TC declaration point [section 2c(2)] in ERA-Interim (Fig. 2b) (dark-gray segments in Fig. 2).
- A "TC track" commences from these points and is terminated when a system either ceases to exist or encounters the STJ (black segments in Fig. 2).
- A "full track" refers to both the initial and TC track segments being taken together.

4. Evaluation of the tracking scheme

a. Inconsistencies between initial tracks

First inspection of the full tracks are quite encouraging as tracks detected by the OWZ scheme (Fig. 2b) are well reproduced compared to the observed records (Fig. 2a). However, a notable discrepancy between the initial tracks is apparent, as ERA-Interim-detected storms appear earlier than they are observed. This is particularly evident just off the western coast of Africa in the NA basin, centrally in the WNP basin, and near the equator in the SH. Figure 3 confirms this earlier detection of TCs by the OWZ scheme as its initial track frequencies exist closer to the equator (within ±10° latitude) and are of longer duration.

This early detection bias is somewhat expected, as conditions favorable for TC development obtained by the OWZ-D's initial parametric thresholds can theoretically precede that of actual observational monitoring of a cyclone (given by meteorological forecast centers). Moreover, possible inconsistencies in the definition of the TC genesis process between forecast-center observational practices (e.g., use of different wind speeds for TC classification and the subjectivity involved in the definition of genesis itself) can also to some extent account for this discrepancy. It is therefore appropriate to remove the initial tracks from further analyses that hereafter focus on our definition of a TC track (section 3b).

b. Validation of TC genesis

As stated earlier in section 2a, we have tried to make the definition of TC genesis (and thus the first-TC-track track point) in IBTrACS as consistent as possible by defining it as the point a TC first reaches a 10-min sustained wind speed of $17\,\mathrm{m\,s^{-1}}$. However, measures of TC intensity (i.e., wind speed and central pressure) are substantially underresolved in ERA-Interim, and therefore the threshold of $17\,\mathrm{m\,s^{-1}}$ cannot be used to define genesis points in storms detected by the OWZ scheme. Notably, the TC declaration point of detected storms was used to represent the TC genesis point in prior studies (Tory et al. 2013b,c,d), to analyze TC formation. However, given those studies used 24-h data and did not worry about tuning to account for any basin

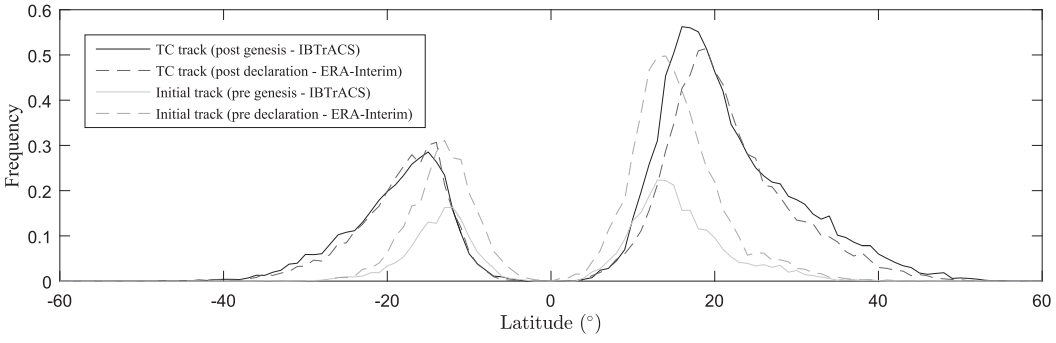

FIG. 3. Latitude position of TC tracks (black) and initial tracks (gray) expressed in terms of a frequency per total storms, rounded to the nearest 1° latitude in IBTrACS (solid lines) and ERA-Interim (dashed lines). Frequencies are (faintly) normalized by the total No. of storms (not by the total No. of track points) in each set.

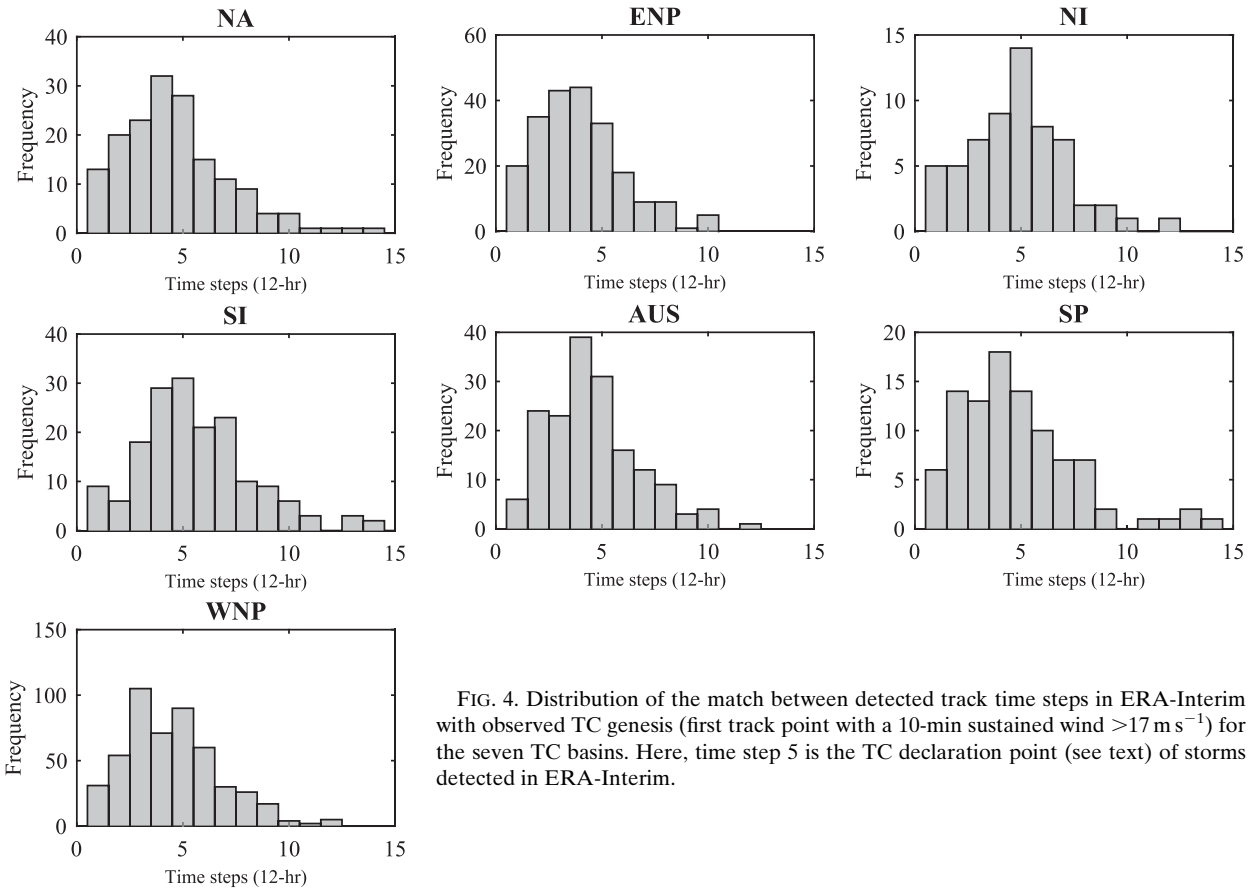

FIG. 4. Distribution of the match between detected track time steps in ERA-Interim with observed TC genesis (first track point with a 10-min sustained wind $>17\,\mathrm{m\,s^{-1}}$) for the seven TC basins. Here, time step 5 is the TC declaration point (see text) of storms detected in ERA-Interim.

differences, it is wise to take this opportunity to validate these points as equivalent when utilizing finer-scale (12 h) data.

This is done by statistically determining which time step along the detected tracks in ERA-Interim most closely matched the TC genesis point in IBTrACS in each of the seven defined basins. Results (Fig. 4) demonstrate that the TC declaration point (fifth time step in Fig. 4) of detected TCs is the most appropriate representation of TC genesis in IBTrACS for all basins. Although, there is potentially room for tuning this in some basins, particularly the ENP basin, where an earlier time period of 12–24 h may be more appropriate.[2] While such an adjustment results in a mild improvement of all statistics for the ENP basin (not shown), a decision was made not to alter our definition of a TC track between basins for the rest of this paper.

[2] Many storms that cross from the Atlantic to the Pacific are quite mature as they reach the warm Pacific waters and as a consequence intensify rapidly to become TCs. The OWZ scheme does not take this into account, and the earliest the TC can be declared is 48 h after the storm reaches the Pacific.

c. *Comparison of TC track clusters*

The objectively defined TC tracks in IBTrACS and ERA-Interim show strong agreement (between mean regressed cluster trajectories) both in terms of geographical location and general shape for most ocean basins around the globe (Fig. 5a). However, the north Indian Ocean Basin is an exception where there is a marked distinction between the respective observed and detected mean trajectories. Prior work with the OWZ scheme (T13B), as well as other studies that used more traditional detection schemes (e.g., Bengtsson et al. 2007; Strachan et al. 2013), has also encountered similar problems here. It should also be noted that the apparent divergence between the first mean trajectories off the coast of Mexico is a cluster-related error. The observed cluster contains storms that originate farther west than the detected cluster. These extra storms bias the observed regression trajectory to take on a trajectory similar to the neighboring westward Mexican cluster.

In addition to climatological comparisons of TC tracks using cluster analysis, further insights on individual observed and detected tracks can be gained from the

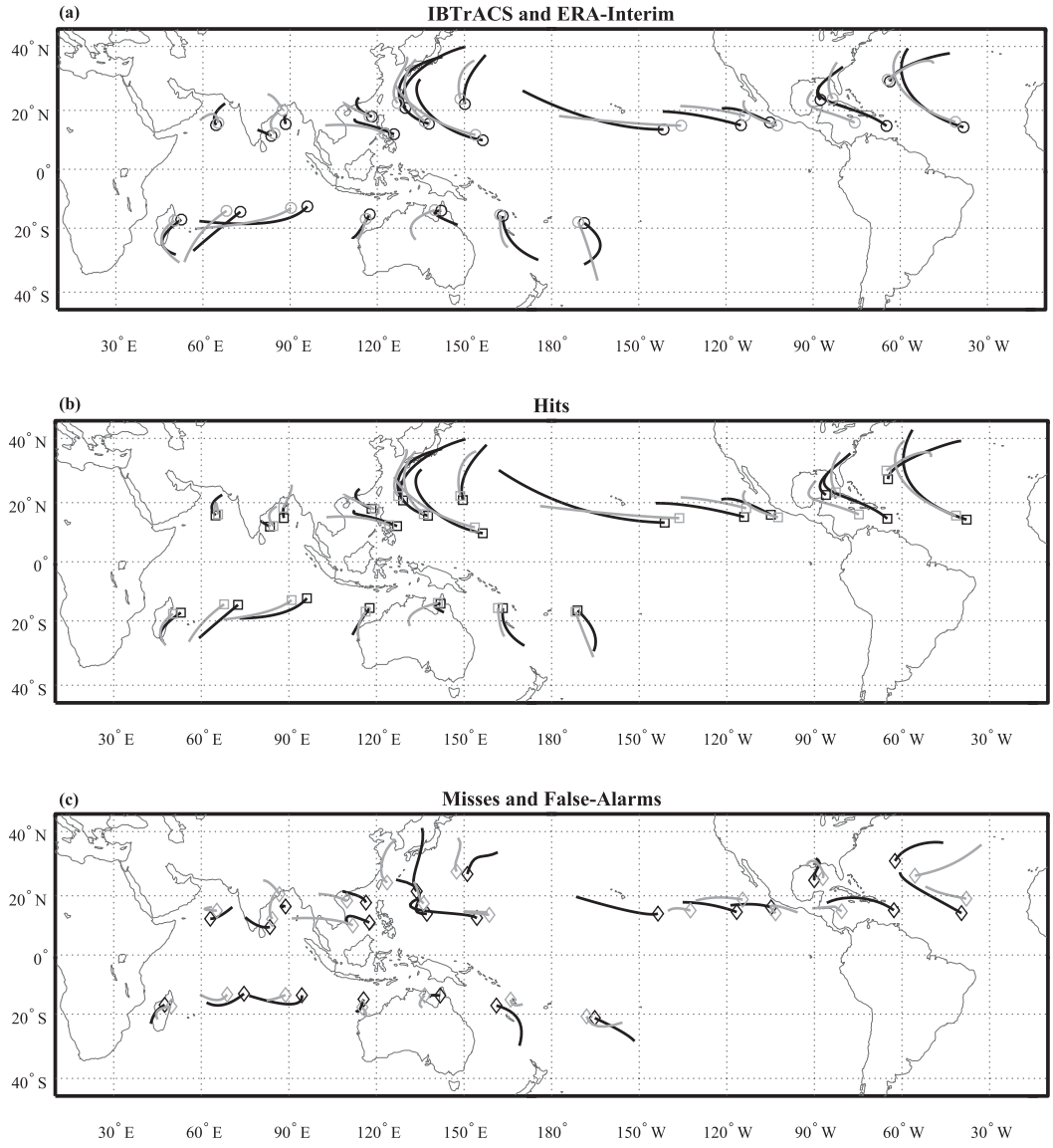

FIG. 5. (a) Mean regression cluster trajectories (length is $\mu + 2\sigma$) of TC tracks as observed in IBTrACS (black lines) with TC genesis point (black circles) and as detected by the OWZ scheme in the ERA-Interim product (gray lines) with TC declaration point (gray circles). (b) As in (a), but the genesis and declaration are now represented by a square, and all TC tracks deemed a hit in each cluster are used to recalculate mean regression trajectories ($\mu + \sigma$). (c) As in (a), but the genesis and declaration points are now represented by a diamond, and all TC tracks deemed a miss in IBTrACS or a false alarm in ERA-Interim, for each cluster, are used to recalculate mean regression trajectories ($\mu + \sigma$).

information derived using the contingency tables of hits, misses, and false alarms (e.g., Table 3). Hit-only clusters (Fig. 5b) are very similar to those in Fig. 5a, indicating a marginal influence of misses and false alarms on the overall trajectories (this is expected as hits consume a much larger proportion, ~80%). Likewise, TC tracks in IBTrACS that were missed by the OWZ scheme in each cluster, and those detected by the scheme but found no match (false alarm) in the same cluster, are also plotted alongside each other (Fig. 5c). It is found most clusters show similar properties, which suggests that, although the false alarms are "errors" of the scheme, to an extent they still represent realistic tracks and compensate for some of the misses in most regions. Exceptions to this can be found in the Coral Sea region (AUS–SP) and off the western coast of Mexico (in the ENP).

Closer examination of some clusters (Fig. 5a) suggests that the OWZ scheme detects a shorter than expected

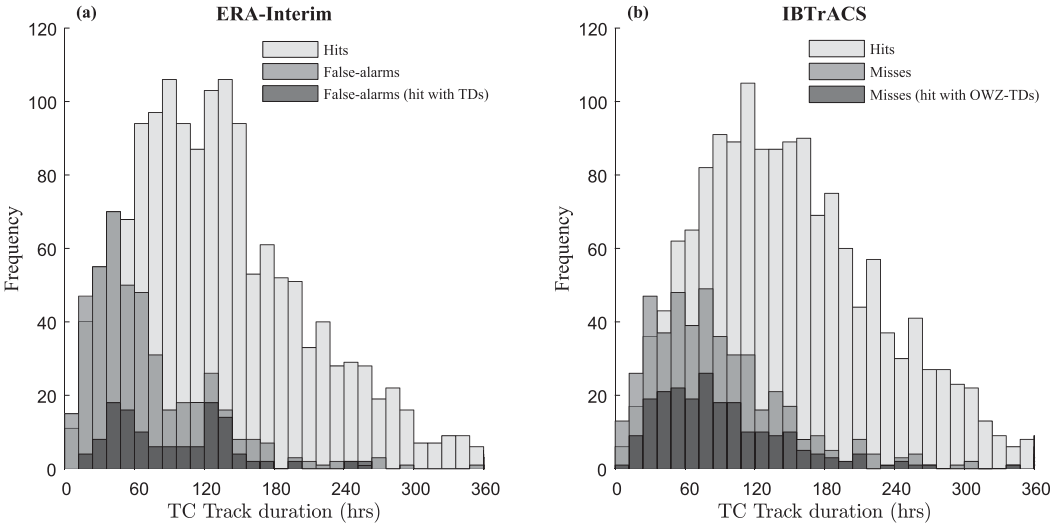

FIG. 6. TC track duration distributions in (a) ERA-Interim of hits, false alarms, and a subset of false alarms that hit with observed TDs and (b) IBTrACS of hits, misses, and a subset of misses that hit with OWZ-detected TDs. Note that the distributions are overlaid with different shades of gray (i.e., frequency values are measured directly off the *y* axis).

track, for example, in the Coral Sea (cluster at ~18°S, 165°E) and also at higher latitudes (two recurving clusters around ~35°–40°N, 135°E) in the WNP. Further analysis (not shown) reveals the detected cluster in the Coral Sea is shortened as a result of that cluster containing a slightly higher frequency of shorter storm tracks. However, the OWZ scheme is still found capable of replicating the longest storm tracks in this cluster realistically. Examination of individual recurving tracks from the aforementioned clusters in the WNP revealed some detected storms to be prematurely terminated. These storms are found to have terminated early because of a reduction in the favorability of their OWZ-D parameters (identified by the core parametric thresholds no longer being met toward the end of their tracks). Alternatively, the increased translational speed here (see section 4h) and sudden change in direction associated with midlatitude steering perhaps leads the expected position (calculated by the tracker by aid of 4° × 4° steering winds) awry and therefore out of its radial range (which also terminates the track).

Overall, it is difficult to pinpoint the precise cause of the small discrepancies in these regions; contributing factors may be subtropical sections of track remaining in IBTrACS and deficiencies in either the reanalysis data or the OWZ scheme itself. Nonetheless, it is an important factor to be aware of in future applications of the OWZ-T.

d. False-alarm-rate sensitivity to track duration

As it was suggested in the prior section that some TC track detections may have a shorter duration than would be expected, this is further investigated by obtaining the duration distributions of both hits and false alarms in ERA-Interim (Fig. 6a) and also hits and misses in IBTrACS (Fig. 6b). While the hit distributions match well, it is found that false alarm TC tracks are skewed toward much shorter durations, even in comparison to the misses, with 41% terminating before reaching 48 h. A subset distribution of false alarms that "hit" with tropical depressions (TDs) from the IBTrACs database[3] are also included (Fig. 6a) and demonstrate that false-alarm TC tracks (>72 h in duration) can be largely attributed to observed TDs. This suggests shorter false-alarm tracks (<72 h in duration) are due to factors other than the subjectivities associated with the 17 m s^{-1} TC threshold; that is, the OWZ scheme is incorrectly activating as a result of tropical disturbances or low-intensity track segments of missed TCs. It could then be argued that, at least in some cases, the OWZ scheme is quick to terminate tracks that are falsely declared TCs.

This leads to potential removal periods based on duration to be considered, with an optimal period to be decided by relative impacts on verification rate measures. These measures are simply the rate (or ratio) of

[3] As there exists no reliable record of observed TDs, the 435 TDs used from 1989 to 2013 in the IBTrACS database are considered incomplete. Over this same period, 922 TDs are detected by the OWZ scheme in ERA-Interim data; therefore, the distribution of false alarms matched with TDs in Fig. 6a is doubled in magnitude to account for the lack of TD observations.

TABLE 5. The impact of different track duration removal periods on the verification rates between TCs in IBTrACS and TCs in ERA-Interim.

Duration removal	Miss rate	False alarm rate
None	0.230	0.228
<12 h	0.232	0.218
<24 h	0.244	0.211
<36 h	0.254	0.209
<48 h	.270	.194
<60 h	0.286	0.204

TABLE 6. Hit rate of TC tracks (at their point of maximum intensity) in IBTrACS with different track types detected in ERA-Interim. Note that the TDs increase the false alarm rate from 23% to 40% (not shown). Full track column values are in boldface as these are indicative of the true hit rate.

	ERA-Interim track type		
Hemisphere	TC track	Full track	TD (full track)
SH	0.688	**.794**	0.889
NH	0.662	**.759**	0.873

false alarms compared to all detections in ERA-Interim [false alarm rate (FAR)] and the rate of misses to all observations in IBTrACS [miss rate (MR)] such that

$$\mathrm{FAR} = \frac{\mathrm{FA}}{\mathrm{FA} + H}, \tag{2}$$

where 1 − FAR is the hit rate of all detections, FA is the number of false alarms, and H is the number of hits, and

$$\mathrm{MR} = \frac{M}{M + H}, \tag{3}$$

where (1 − MR) is the hit rate of all observations and M is the number of misses.

The impact of removing short-term TC tracks (from <12 to <60 h) in duration on these rates are provided in Table 5, with a removal period of less than 48 h found to minimize the false alarm rate (19.4%). It is also noted that the false alarm rate decreases further (to 16.5% at a 48-h removal) if short-term duration observed TC tracks are not removed, as some (>48 h) false alarms hit with (<48 h) observations. Naturally this also increases the miss rate from 27% to 32%.

Although overall performance is decreased (i.e., miss rate increases slightly more than false alarm rate decreases) such a removal would produce a more reliable track climatology. This removal could then extend to climate model applications where detected TC tracks could be objectively excluded based on their duration to improve performance.

e. Hit-rate sensitivity to track type

A preceding work (T13B) has provided a detailed statistical assessment of the frequency of verification measures (e.g., hit and false alarm rates). They also found that over 90% of observed TCs that reached at least category 3 intensity are correctly identified. This section instead looks at how sensitive the hit rate of TCs in IBTrACS is to the type of track chosen in ERA-Interim (note the criterion for a hit is slightly altered between studies). If a TC in IBTrACS is successfully detected in ERA-Interim, it is sensible to assume that this detected storm should be within a 3.5° radius of the observed TC when it reaches its peak intensity (as per our definition of a hit in section 2e).

The hit rate between three different detected track types (TC track, full track, and a TD full track) and TCs observed in IBTrACS are given in Table 6. TDs are detected in ERA-Interim by the OWZ scheme with a less strict 24-h core criterion period before declaration (compared to 48 h for TCs). Results show full tracks achieve a boost in hit rate of around 10% compared to the TC tracks. This means that the track point in ERA-Interim analogous to the maximum intensity point in IBTrACS occurs before declaration, or in other words during the initial track of a detected storm around 10% of the time in both hemispheres. This can be partially explained by lower-category storms in IBTrACS sometimes reaching a maximum intensity on the same point that they achieve TC genesis (first point >17 m s^{-1}). In accordance with this, the full track column values in Table 6 are in boldface as these are indicative of the true hit rate. Furthermore, full tracks of "OWZ-TDs" (marginally not declared TCs by the OWZ-D) boost the hit rate by an additional 10%. This highlights the subjectivity involved in defining a TC from a non-TC with a somewhat arbitrary wind speed threshold.

f. Haversine distance measure

Note that for this section, and in section 4h, tracks have been cut off at a fixed 40° latitude and not the STJ. As a hit is composed of both an observed TC track and a corresponding TC track in ERA-Interim, a haversine distance can be computed between the respective track points that occur on the same date. Measuring this may provide some insight into the biases between a TC's real-world position and its position detected in ERA-Interim by the OWZ scheme. Such biases may arise from meteorological centers having the luxury of satellite imagery to accurately pinpoint TC coordinates, in contrast to the OWZ-D that relies on the averaged position between favorable 1° × 1° grid points

TABLE 7. MHD between corresponding (hit) TC tracks in IBTrACS and ERA-Interim. Computed at the same date and time and also at a lead (−12 h) and lag (+12 h) in the reanalysis, for the seven TC basins. Given in degrees latitude.

	MHD (lat)		
Basin	Same date and time	−12 h	+12 h
NA	0.73°	2.11°	1.80°
ENP	1.00°	2.02°	1.47°
WNP	0.73°	2.09°	1.88°
NI	1.05°	1.60°	1.36°
SP	1.04°	1.80°	1.82°
AUS	0.89°	1.71°	1.49°
SI	0.97°	2.24°	1.47°

within a circulation to render its coordinates (see also section 2e).

Haversine distance determines the great circle distance between two points on a sphere (Earth's surface is approximated as a sphere here) given their geographical locations in terms of latitudes and longitudes (e.g., Terry and Gienko 2011). In our case, the mean haversine distance (MHD) for each basin is obtained by calculating an average haversine distance for each TC in a basin and then accumulating it for all TCs over the basin under consideration, such that

$$\mathrm{MHD} = \frac{\sum_{i=1}^{N}\sum_{t=0}^{L}|D(t)|}{N(\sum L)}, \tag{4}$$

where $|D(t)|$ is the absolute haversine distance between the coordinates (in degrees), L is the number of same-date-matched track points in an individual TC track, and N is the total number of TC tracks in a specific basin. A value of zero indicates a perfect match; the more the deviation from zero, the more the bias.

MHDs values range from 0.73° to 1.05° (Table 7), which are all within the expected ranges given the ERA-Interim data themselves are on a 1° × 1° grid. Moreover, in order to ensure that the favorable conditions detected by OWZ-D are not lagging (or leading) the actual observations, MHD values are calculated at a 12-h (i.e., one time step) lead and lag. Uniformly larger MHD values for the lead and lag steps, compared to the zero-lag cases, are obtained indicating that circulations detected by OWZ-D most closely resemble their observed counterparts (i.e., no predominant ~12-h lead or lag is present in the OWZ-D).

The focus thus far has been on the overall shape and direction of propagation of TCs in IBTrACS and ERA-Interim using various statistical measures. In the next two sections, we assess the OWZ scheme's ability to replicate two other TC track characteristics: tropical cyclone lifetime (measured in terms of TC days) and translational speeds.

g. TC days

The frequency of TC tracks and their lifetimes can be represented using a single parameter called TC days (TCDAYS). The annual (or seasonal) number of TCDAYS is defined here as the number of 12-h periods during which an active TC occurs within a basin, divided by 2 (to convert 12-h blocks into days) and accumulated for the season under consideration such that

$$\mathrm{TCDAYS} = \frac{1}{2}\sum_{i=1}^{N} L_i, \tag{5}$$

where L_i is the individual lifetime of a TC within the bounds of a basin. Note that in this study, a TC season in any NH basin is the entire calendar year (i.e., from January to December), whereas for the SH basins, a TC season is spread over two calendar years (i.e., from July of the first year to June of the second year) and is referred to using the overlapping year format (e.g., 2001/02).

We assess the ability of the OWZ scheme to accurately replicate the observed interannual TCDAYS over the period 1989–2013 across the seven TC basins. Figure 7 shows the relationship between TCDAYS in the observed records (solid lines) and that detected (dashed lines) for the different basins. Statistically significant results (as evaluated using Pearson's correlation coefficients with 23 degrees of freedom in this case) are found for most basins (correlation coefficients range from 0.338 for the north Indian Ocean to 0.923 for the North Atlantic). Correlations are also provided for alternative track cutoff points (i.e., 20°, 30°, and 40° latitude) and are found to show limited sensitivity outside of the NI Basin.

Decomposing the TCDAYS data into hits, misses, and false alarms (Fig. 8) reveals that the weaker relationship in the north Indian Ocean Basin is mostly due to consistent false alarms (gray dashed) in this basin, while the overestimation of hits (black dashed) only occurs in this and the AUS basin. Notably, these two basins share the trait of detected systems being tracked too far over land (Fig. 2b). If this also occurs in climate model applications, and is not a by-product specific to ERA-Interim, tracks may need to be manually terminated for such cases.

h. Translational speed

The speed at which a TC moves from one geographical location to another is termed its translational

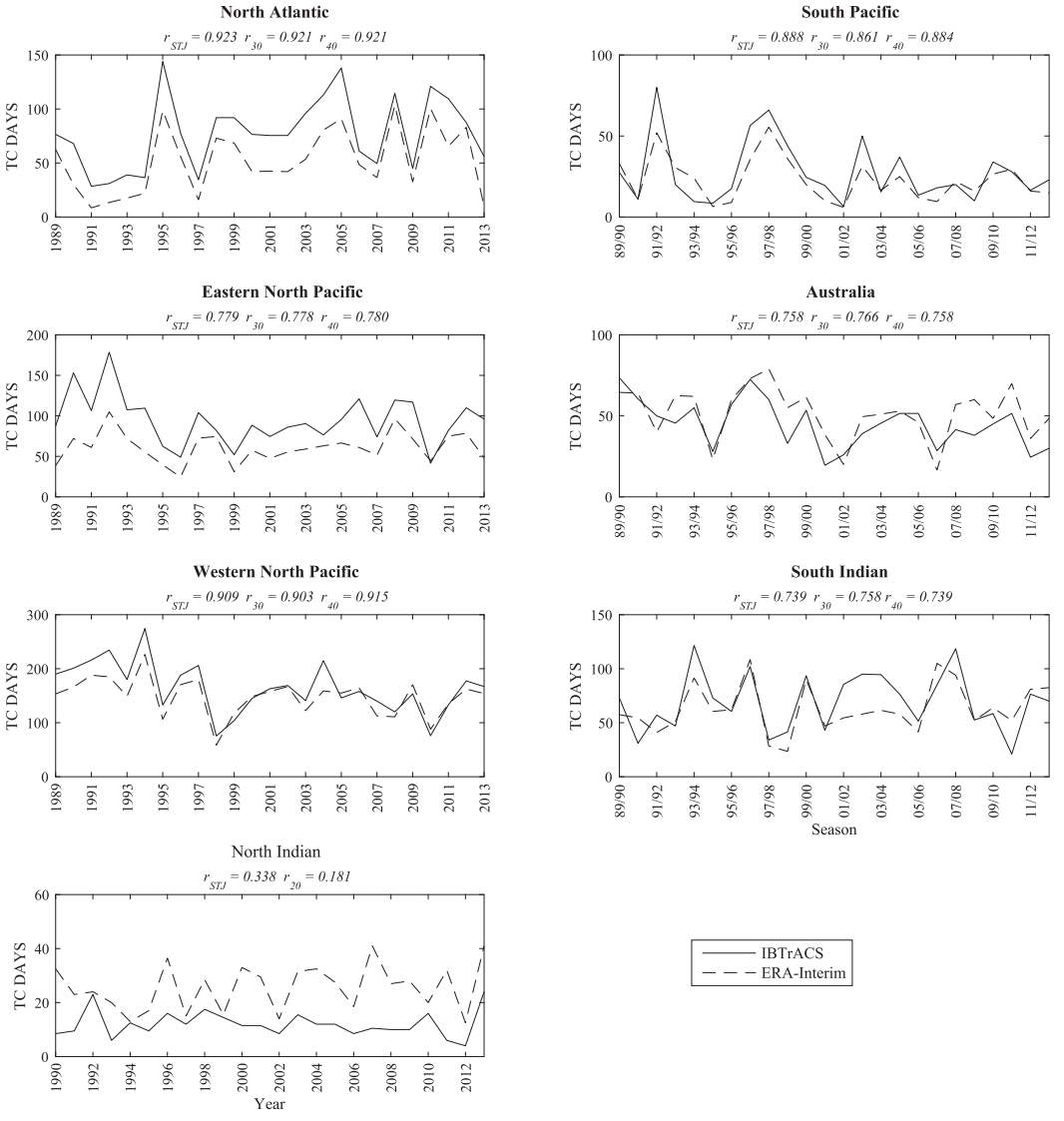

FIG. 7. TCDAY interannual variation for all TCs in IBTrACS (solid lines) and ERA-Interim (dashed lines), using annual period definitions for NH (1989–2013) and SH (1989/90–2012/13). Underneath each basin title is the correlation coefficients r between interannual TCDAY numbers at several different track cutoff points (STJ and 30°, 40°, and 20° lat), with basin titles in boldface to indicate significance of the STJ correlation at the 95% level.

speed. In this study, the mean translational speed is calculated by first determining the total haversine distance for each TC in a basin, accumulating it over all TCs for that basin, and then dividing the result by respective TCDAYS such that

$$\text{mean translational speed} = \frac{\sum_{i=1}^{N}\sum_{t=0}^{L}|D(t)|}{\frac{1}{2}\sum_{i=1}^{N}L_i}. \qquad (6)$$

Note that the translational speed of a TC may be affected by different large-scale conditions in the tropics and nontropics. For example, TC movement in the latter may be influenced by adiabatic baroclinicity (e.g., Wu and Wang 2001). For this reason, each basin is divided here into two zones: zone 1 (0°–24° latitude), which captures largely tropical conditions, and zone 2 (24°–40° latitude), which roughly captures the edge of the tropics and the beginning of the midlatitudes (tracks analyzed here are not cutoff by the STJ). Overall, the translational speed of TCs in the IBTrACS and ERA-Interim

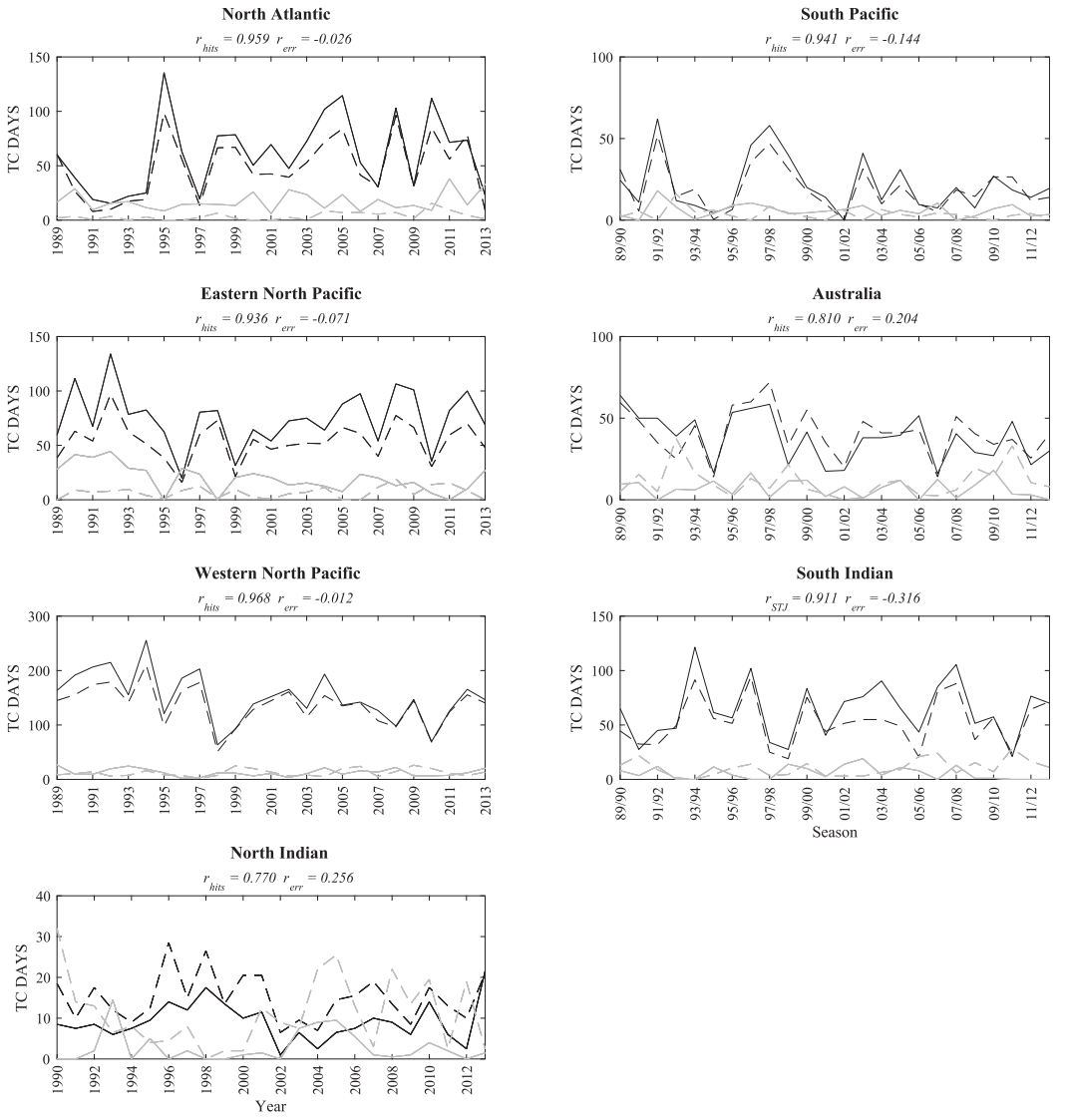

FIG. 8. Decomposition of Fig. 7 by verification. IBTrACS (solid lines) for hits (black) and misses (gray) and ERA-Interim (dashed lines) for hits (black), and false alarms (gray). Correlation between hits r_{hits} and misses or false alarms r_{err} are shown below each basin title. Boldface basin titles indicates significance of the hit correlation at the 95% level.

are very similar, indicating that this parameter is also well captured by the OWZ scheme (Table 8).

5. Summary and concluding remarks

The performance of the OWZ tracking scheme was evaluated on the ERA-Interim data in order to uncover any potential biases that may affect its application to climate models. Various statistical measures were used to compare the observed tracks in the IBTrACS database to those detected in ERA-Interim by the OWZ scheme over the period 1989–2013 for different TC basins.

For the purpose of this study, we objectively defined a "TC track" as follows.

- In IBTrACS, a TC track is referred to as the track from the point of genesis (i.e., the point where a TC first reaches the 10-min sustained wind speed of $17\,\text{m}\,\text{s}^{-1}$) to the point where a TC either ceases to exist or encounters the STJ.
- In ERA-Interim, a TC track referred to the track from the point of TC declaration (five consecutive core criterion passes) identified by the OWZ scheme to the point where a TC either ceases to exist or encounters the STJ.

TABLE 8. Mean TC translational speeds (km h^{-1}) along TC tracks in the seven TC basins and in two separate zones: zone 1 (0°–24° lat) and zone 2 (24°–40° lat) in IBTrACS and ERA-Interim. Boldface values indicate distributions are significantly similar at 95%. The r^2 values are from regressing the MHDs of same date and time TC track hits.

	Translational speed (km h^{-1})					
	Zone 1			Zone 2		
Basin	IBTrACS	ERA-Interim	r^2	IBTrACS	ERA-Interim	r^2
NA	**16.3**	**17.3**	0.94	**18.6**	**18.0**	0.94
ENP	**14.3**	**15.1**	0.86	**12.0**	**12.4**	0.82
WNP	**14.7**	**14.5**	0.87	24.4	21.2	0.94
NI	**11.3**	**12.1**	0.75	**10.8**	**11.0**	0.71
SP	**14.3**	**15.2**	0.82	**25.6**	**24.1**	0.90
AUS	**12.4**	**13.4**	0.84	**20.1**	**16.9**	0.91
SI	**12.6**	**12.4**	0.72	**18.7**	**19.2**	0.89

Cluster analysis of all TC tracks revealed strong similarities in geographical location and general shape pattern of mean track trajectories for most ocean basins around the globe, with an exception of the north Indian Ocean Basin where past studies have also indicated some inconsistencies. Comparisons improved further when only hit cases were considered in the analysis; however, the impact of false alarms on the climatology was small as they were shown to exhibit largely realistic trajectories and compensated for some of the misses. A minimum TC track duration cap of 48 h was found to remove a large amount of false alarms, particularly those that were less likely to be attributed to TDs, producing a trade-off between increased misses and decreased false alarms. Track coordinate deviation fell within the expected range, while a predominant lead or lag of the OWZ-D was not found. Other TC track characteristics were also evaluated, particularly TCDAYS and translational speed. Results indicated substantial ability of the OWZ scheme to reproduce these characteristics in ERA-Interim. This gives us confidence in the scheme for its application to climate models simulations, which we will be examining in our subsequent studies.

Acknowledgments. We thank Andrew Dowdy and Paul Gregory for their insights. We acknowledge that this work was partly supported by an Australian Government Research Training Program (RTP) Scholarship. We also acknowledge further support from the Australian Government's National Environmental Science Programme (NESP).

REFERENCES

Bengtsson, L., M. Botzet, and M. Esch, 1995: Hurricane-type vortices in a general circulation model. *Tellus*, **47A**, 175–196, https://doi.org/10.3402/tellusa.v47i2.11500.

——, K. I. Hodges, and M. Esch, 2007: Tropical cyclones in a T159 resolution global climate model: Comparison with observations and re-analyses. *Tellus*, **59A**, 396–416, https://doi.org/10.1111/j.1600-0870.2007.00236.x.

Camargo, S. J., 2013: Global and regional aspects of tropical cyclone activity in the CMIP5 models. *J. Climate*, **26**, 9880–9902, https://doi.org/10.1175/JCLI-D-12-00549.1.

——, A. W. Robertson, S. J. Gaffney, P. Smith, and M. Ghil, 2007: Cluster analysis of typhoon tracks. Part I: General properties. *J. Climate*, **20**, 3635–3653, https://doi.org/10.1175/JCLI4188.1.

——, ——, A. G. Barnston, and M. Ghil, 2008: Clustering of eastern North Pacific tropical cyclone tracks: ENSO and MJO effects. *Geochem. Geophys. Geosyst.*, **9**, Q06V05, https://doi.org/10.1029/2007GC001861.

Chan, J. C. L., and W. M. Gray, 1982: Tropical cyclone movement and surrounding flow relationships. *Mon. Wea. Rev.*, **110**, 1354–1374, https://doi.org/10.1175/1520-0493(1982)110<1354:TCMASF>2.0.CO;2.

Chand, S. S., and K. J. E. Walsh, 2009: Tropical cyclone activity in the Fiji region: Spatial patterns and relationship to large-scale circulation. *J. Climate*, **22**, 3877–3893, https://doi.org/10.1175/2009JCLI2880.1.

Chauvin, F., J.-F. Royer, and M. Deque, 2006: Response of hurricane type vortices to global warming as simulated by ARPEGE-Climat at high resolution. *Climate Dyn.*, **27**, 377–399, https://doi.org/10.1007/s00382-006-0135-7.

Daloz, A. S., and Coauthors, 2015: Cluster analysis of downscaled and explicitly simulated North Atlantic tropical cyclone tracks. *J. Climate*, **28**, 1333–1361, https://doi.org/10.1175/JCLI-D-13-00646.1.

Dee, D. P., and Coauthors, 2011: The ERA-Interim reanalysis: Configuration and performance of the data assimilation system. *Quart. J. Roy. Meteor. Soc.*, **137**, 553–597, https://doi.org/10.1002/qj.828.

Dunkerton, T. J., M. T. Montgomery, and Z. Wang, 2009: Tropical cyclogenesis in a tropical wave critical layer: Easterly waves. *Atmos. Chem. Phys.*, **9**, 5587–5646, https://doi.org/10.5194/acp-9-5587-2009.

Gaffney, S. J., 2004: Probabilistic curve-aligned clustering and prediction with regression mixture models. Ph.D. thesis, University of California, Irvine, 281 pp., http://www.ics.uci.edu/pub/sgaffney/outgoing/sgaffney_thesis.pdf.

——, A. W. Robertson, P. Smyth, S. J. Camargo, and M. Ghil, 2007: Probabilistic clustering of extratropical cyclones using regression mixture models. *Climate Dyn.*, **29**, 423–440, https://doi.org/10.1007/s00382-007-0235-z.

Harper, B. A., J. D. Kepert, and J. D. Ginger, 2010: Guidelines for converting between various wind averaging periods in tropical cyclone conditions. WMO Tech. Doc. 1555, 64 pp., https://www.wmo.int/pages/prog/www/tcp/documents/WMO_TD_1555_en.pdf.

Hart, R. E., and J. L. Evans, 2001: A climatology of the extratropical transition of Atlantic tropical cyclones. *J. Climate*, **26**, 5493–5507, https://doi.org/10.1175/1520-0442(2001)014<0546:ACOTET>2.0.CO;2.

Horn, M., and Coauthors, 2014: Tracking scheme dependence of simulated tropical cyclone response to idealized climate simulations. *J. Climate*, **27**, 9197–9213, https://doi.org/10.1175/JCLI-D-14-00200.1.

Knapp, K. R., M. C. Kruk, D. H. Levinson, H. J. Diamond, and C. J. Neumann, 2010a: The International Best Track Archive for Climate Stewardship (IBTrACS) unifying tropical cyclone data. *Bull. Amer. Meteor. Soc.*, **91**, 363–376, https://doi.org/10.1175/2009BAMS2755.1.

——, S. Applequist, H. J. Diamond, J. P. Kossin, M. Kruk, and C. Schreck, 2010b: NCDC International Best Track Archive for Climate Stewardship (IBTrACS) Project, version 3. NOAA National Centers for Environmental Information. Subset used: January 1989–December 2013, accessed 12 August 2016, https://doi.org/10.7289/V5NK3BZP.

Kossin, J. P., S. J. Camargo, and M. Sitkowski, 2010: Climate modulation of North Atlantic hurricane tracks. *J. Climate*, **23**, 3057–3076, https://doi.org/10.1175/2010JCLI3497.1.

——, K. A. Emanuel, and G. A. Vecchi, 2014: The poleward migration of the location of tropical cyclone maximum intensity. *Nature*, **509**, 349–352, https://doi.org/10.1038/nature13278.

Okubo, A., 1970: Horizontal dispersion of floatable particles in the vicinity of velocity singularities such as convergences. *Deep-Sea Res.*, **17**, 445–454, https://doi.org/10.1016/0011-7471(70)90059-8.

Paliwal, M., and A. Patwardhan, 2013: Identification of clusters in tropical cyclone tracks of north Indian Ocean. *Nat. Hazards*, **68**, 645–656, https://doi.org/10.1007/s11069-013-0641-y.

Ramsay, H. A., S. J. Camargo, and D. Kim, 2012: Cluster analysis of tropical cyclone tracks in the Southern Hemisphere. *Climate Dyn.*, **39**, 897–917, https://doi.org/10.1007/s00382-011-1225-8.

Romero-Vadillo, E., O. Zaytsev, and R. Morales-Pérez, 2007: Tropical cyclone statistics in the northeastern Pacific. *Atmósfera*, **20**, 197–213.

Sinclair, M. R., 2002: Extratropical transition of southwest Pacific tropical cyclones. Part I: Climatology and mean structure changes. *Mon. Wea. Rev.*, **130**, 590–609, https://doi.org/10.1175/1520-0493(2002)130<0590:ETOSPT>2.0.CO;2.

Strachan, J. P., L. Vidale, K. Hodges, M. Roberts, and M.-E. Demory, 2013: Investigating global tropical cyclone activity with a hierarchy of AGCMs: The role of model resolution. *J. Climate*, **26**, 133–152, https://doi.org/10.1175/JCLI-D-12-00012.1.

Taylor, K. E., R. J. Stouffer, and G. A. Meehl, 2012: An overview of CMIP5 and the experimental design. *Bull. Amer. Meteor. Soc.*, **93**, 485–498, https://doi.org/10.1175/BAMS-D-11-00094.1.

Terry, J. P., and G. Gienko, 2011: Developing a new sinuosity index for cyclone tracks in the tropical South Pacific. *Nat. Hazards*, **59**, 1161–1174, https://doi.org/10.1007/s11069-011-9827-3.

Tory, K. J., and R. A. Dare, 2015: Sea surface temperature thresholds for tropical cyclone formation. *J. Climate*, **28**, 8171–8183, https://doi.org/10.1175/JCLI-D-14-00637.1.

——, ——, N. E. Davidson, J. L. McBride, and S. S. Chand, 2013a: The importance of low-deformation vorticity in tropical cyclone formation. *Atmos. Chem. Phys.*, **13**, 2115–2132, https://doi.org/10.5194/acp-13-2115-2013.

——, S. S. Chand, R. A. Dare, and J. L. McBride, 2013b: The development and assessment of a model-, grid-, and basin-independent tropical cyclone detection scheme. *J. Climate*, **26**, 5493–5507, https://doi.org/10.1175/JCLI-D-12-00510.1.

——, ——, ——, and ——, 2013c: An assessment of a model-, grid-, and basin-independent tropical cyclone detection scheme in selected CMIP3 global climate models. *J. Climate*, **26**, 5508–5522, https://doi.org/10.1175/JCLI-D-12-00511.1.

——, ——, J. L. McBride, H. Ye, and R. A. Dare, 2013d: Projected changes in late-twenty-first-century tropical cyclone frequency in 13 coupled climate models from phase 5 of the Coupled Model Intercomparison Project. *J. Climate*, **26**, 9946–9959, https://doi.org/10.1175/JCLI-D-13-00010.1.

——, ——, ——, ——, and ——, 2014: Projected changes in late 21st century tropical cyclone frequency in CMIP5 models. *Proc. 31st Conf. on Hurricanes and Tropical Meteorology*, San Diego, CA, Amer. Meteor. Soc., https://ams.confex.com/ams/31Hurr/webprogram/Paper245100.html.

——, H. Ye, and R. A. Dare, 2018: Understanding the geographic distribution of tropical cyclone formation for applications in climate models. *Climate Dyn.*, https://doi.org/10.1007/s00382-017-3752-4, in press.

Walsh, K. J. E., M. Fiorino, C. W. Landsea, and K. L. McInnes, 2007: Objectively determined resolution-dependent threshold criteria for the detection of tropical cyclones in climate models and reanalyses. *J. Climate*, **20**, 2307–2314, https://doi.org/10.1175/JCLI4074.1.

——, and Coauthors, 2016: Tropical cyclones and climate change. *Wiley Interdiscip. Rev.: Climate Change*, **7**, 65–89, https://doi.org/10.1002/wcc.371.

Weiss, J., 1991: The dynamics of enstrophy transfer in two-dimensional hydrodynamics. *Physica D*, **48**, 273–294, https://doi.org/10.1016/0167-2789(91)90088-Q.

Wu, L., and B. Wang, 2001: Movement and vertical coupling of adiabatic baroclinic tropical cyclones. *J. Atmos. Sci.*, **58**, 1801–1814, https://doi.org/10.1175/1520-0469(2001)058<1801:MAVCOA>2.0.CO;2.